J Physiol Sci (2018) 68:377–385
https://doi.org/10.1007/s12576-017-0540-1

ORIGINAL PAPER

The central clock controls the daily rhythm of *Aqp5* expression in salivary glands

Hitoshi Uchida[1,2] · Takahiro J. Nakamura[3,4] · Nana N. Takasu[1] · Aya Obana-Koshino[2] · Hitomi Ono[2] · Takeshi Todo[5] · Takayoshi Sakai[2] · Wataru Nakamura[1]

Received: 11 March 2017 / Accepted: 20 April 2017 / Published online: 8 May 2017

Abstract Salivary secretion displays day–night variations that are controlled by the circadian clock. The central clock in the suprachiasmatic nucleus (SCN) regulates daily physiological rhythms by prompting peripheral oscillators to adjust to changing environments. Aquaporin 5 (*Aqp5*) is known to play a key role in salivary secretion, but the association between *Aqp5* and the circadian rhythm is poorly understood. The aim of our study was to evaluate whether *Aqp5* expression in submandibular glands (SMGs) is driven by the central clock in the SCN or by autonomous oscillations. We observed circadian oscillations in the activity of period circadian protein homolog 2 and luciferase fusion protein (PER2::LUC) in cultured SMGs with periodicity depending on core clock genes. A daily rhythm was detected in the expression profiles of *Aqp5* in SMGs in vivo. In cultured SMGs ex vivo, clock genes showed distinct circadian rhythms, whereas *Aqp5* expression did not. These data indicate that daily *Aqp5* expression in the mouse SMG is driven by the central clock in the SCN.

✉ Wataru Nakamura
wataru_nakamura@nagasaki-u.ac.jp

[1] Department of Oral-Chrono Physiology, Nagasaki University Graduate School of Biomedical Sciences, 1-7-1 Sakamoto, Nagasaki, Nagasaki 852-8588, Japan

[2] Department of Oral-Facial Disorders, Graduate School of Dentistry, Osaka University, Suita, Osaka 565-0871, Japan

[3] Department of Life Sciences, School of Agriculture, Meiji University, Kawasaki, Kanagawa 214-8571, Japan

[4] Faculty of Pharmaceutical Sciences, Teikyo Heisei University, Tokyo 164-8530, Japan

[5] Department of Radiation Biology and Medical Genetics, Graduate School of Medicine, Osaka University, Suita, Osaka 565-0871, Japan

Keywords Circadian rhythm · Salivary gland · Suprachiasmatic nucleus · Aquaporin 5 · Period 2

Introduction

Saliva is essential for the maintenance of oral homeostasis [1, 2] and contains various enzymes and growth factors [3, 4]. In humans, saliva is secreted from three major glands, namely, the parotid glands, sublingual glands, and submandibular glands (SMGs), as well as other minor glands [5]. Saliva secretion is regulated by the autonomic nervous system through different mechanisms. For example, sympathetic stimulation greatly increases salivary protein concentration while lowering the flow rate, while parasympathetic stimulation triggers an abundant flow of saliva with a lower protein concentration [6–8]. The flow rate and components of unstimulated human saliva display diurnal rhythms, with the secretory volume increasing during the day in the active phase and decreasing at night during the resting phase [9]. The concentrations of epithelial growth factor and nerve growth factor [10], as well as adrenergic receptor density [11], also show diurnal rhythms in the SMGs of mice.

Previous studies have shown that aquaporins (AQPs) play an important role in regulating water permeability in salivary secretion. AQPs form a family of membrane water channels that primarily function to transport water across the plasma membrane. To date, 13 members of this family (AQP0–AQP12) have been identified in mammals [12–14], among which AQP1, AQP4, AQP5, and AQP8 are expressed in the salivary glands [15]. Previous studies have demonstrated that pilocarpine stimulation induces a 40% increase in saliva release from AQP5 null mice compared with wild-type (WT) mice, although the secretion of

proteins such as amylase was not affected [16, 17]. The AQP5 is one of the major molecules related to saliva secretion, and it has therefore been suggested that AQP5 is associated with the diurnal rhythms of unstimulated saliva secretion.

The central circadian pacemaker, a cluster of hypothalamic neurons located in the suprachiasmatic nucleus (SCN) of the hypothalamus, regulates various physiological functions [18]. Circadian oscillators are also located in other brain regions outside the SCN [19, 20], as well as in peripheral tissues [21–23]. A hierarchical architecture in the circadian system has been proposed in which each peripheral clock oscillates with intrinsic circadian periodicities, with the SCN synchronizing the timing of these peripheral oscillators via neuronal and humoral pathways [24]. Studies have shown that experimental isolation or blockade of the central clock output interrupts circadian rhythms at various levels of physiology, underscoring the importance of the SCN as a circadian pacemaker [25–27].

The circadian oscillations in individual cells are composed of interacting positive and negative transcriptional–translational feedback loops (TTFLs) involving the BMAL1-CLOCK transcriptional activator complex and their target genes which are members of the period (*Per1*, *Per2*, *Per3*) and cryptochrome (*Cry1*, *Cry2*) family of circadian clock genes, respectively [24]. The corresponding proteins (PER1, PER2, PER3 and CRY1 and CRY2) act as negative regulators that suppress the activity of BMAL1-CLOCK. *Cry1* and *Cry2* have been found to be required for normal circadian rhythms: $Cry1^{-/-}$ $Cry2^{-/-}$ mice exhibit arrhythmic behavior in constant darkness [28]. In the mouse SMG, expression of clock genes shows circadian variation in vivo [21, 29, 30], suggesting that the SMG has an intrinsic molecular oscillation system. It has also been speculated that this local molecular clock regulates the circadian rhythm of saliva secretion [30].

The aim of the study reported here was to determine whether the circadian expression of *Aqp5*, an important molecule regulating water permeability in salivary secretion, is driven by the master clock in the SCN or whether it is regulated by the autonomous molecular clock in the SMG. We examined expression levels of the clock genes *Per2* and *Bmal1*, the clock-controlled gene *Dbp*, and *Aqp5* in the SMGs of mice in vivo and compared the expression profiles of these genes with those in isolated SMG cultures ex vivo.

Materials and methods

Ethics statement

This study was carried out in strict accordance with the laws and notifications of the Japanese government. The protocol was approved by the Animal Care and Use Committee at Osaka University (permission# AD-20-042). All tissue sampling was performed with the animals under anesthesia, and all efforts were made to minimize suffering.

Animals

Knock-in mice expressing the PERIOD2::LUCIFERASE fusion protein (PER2::LUC; [23]) and $Cry1^{-/-}$, $Cry2^{-/-}$ and $Cry1^{-/-}Cry2^{-/-}$ mice [28] were used in this study. PER2::LUC mice were purchased from the Jackson Laboratory (Strain#006852; Bar Harbor, ME USA). $Cry1^{+/-}$ *and* $Cry2^{+/-}$mice were backcrossed with the C57BL/6J Jms Slc strain for ten generations and bred with PER2::-LUC mice carrying a PER2 fusion luciferase reporter. These were intercrossed to generate $Cry1^{-/-}$and $Cry2^{-/-}$ mice with a heterozygous *Per2*::*Luc* gene [20]. Animals were housed in groups and kept under a light regimen of 12 h of light and 12 h of darkness [lights on at 0800 hours; lights off at 2000 hours; lights off was defined as Zeitgeber time (ZT) 12]. Food and water were available ad libitum.

Bright-field and bioluminescence imaging

Male 3-month-old heterozygous PER2::LUC mice were euthanized by cervical dislocation at ZT 7. The SMG was rapidly removed, placed in ice-cold Hank's buffered salt solution (HBSS) and then sliced into 50-μm thick sections using a D.S.K LinearSlicer PRO 7 (Dosaka EM Co., Ltd, Kyoto, Japan). SMG slices were placed onto MilliCell-CM Culture Plate Inserts (PICM ORG 50; Millipore, Billerica, MA) in a 35-mm plastic dish (1000-035; IWAKI, Tokyo, Japan) containing 1.2 mL of recording medium [Dulbecco's Modified Eagle Medium (Life Technologies, Carlsbad, CA) supplemented with 7.5% sodium bicarbonate solution, 10 mM HEPES, 25 U/mL penicillin, 25 μg/mL streptomycin, B27 supplement (Life Technologies), and 0.1 mM luciferin]. Dishes were sealed with a gas-permeable FEP film 25F (0803-18-16-11; TGK Co., Ltd., Tokyo, Japan) using silicone grease (G-40 M; Shin-Etsu Chemical Co., Ltd., Tokyo, Japan). Bright-field images and bioluminescence images were acquired according to previously reported procedures [31]. Briefly, images from SMG slices were captured using an ImagEM Enhanced EM-CCD camera (Hamamatsu Photonics, Hamamatsu, Japan; frame rate 32 frames/s; EM gain 1200; objective lens; UPlanSApo ×10, NA 0.40; Olympus, Tokyo, Japan) in a light-tight 36.0 °C environmental chamber. The bioluminescence images were stored as consecutive 50-s summed images every 1 min for 3 days, with recording starting at ZT 12. Pseudocoloring was applied to

PER2::LUC images using ImageJ software (http://imagej.nih.gov/ij/).

Real–time monitoring of bioluminescence in cultured SMGs

Male 2–3 month-old WT, *Cry1*$^{-/-}$, and *Cry2*$^{-/-}$ mice carrying the PER2::LUC allele were euthanized by cervical dislocation under anesthesia at ZT 12, and the SMG was rapidly dissected, trimmed to 2-mm thickness, and processed in the same manner as previously described [32]. SMG sections were maintained in the dark in an incubator at 35 °C and continuously monitored with a photomultiplier tube (Hamamatsu Photonics K.K., Shizuoka, Japan) for 7 days ($n = 8$ mice of each genotype). Bioluminescence data were analyzed as previously described [20, 33] with a slight modification. Briefly, bioluminescence data were determined by detrending (a 24-h moving average was subtracted from the raw data) and smoothing (using a 3-h moving average) of the raw data. In this smoothed data, the acrophase was determined as the highest point that occurred between 18 and 42 h after the start of bioluminescence recording. The period of PER2::LUC activity was calculated by averaging the periods between each consecutive peak from the first four peaks of the smoothed data.

SMG tissue collection at six time points

For in vivo experiments, male and female 2- to 9-month-old WT and *Cry1*$^{-/-}$ *Cry2*$^{-/-}$ mice were euthanized by cervical dislocation under anesthesia, and SMGs were rapidly dissected at six different time points: ZT 4, 8, 12, 16, 20, and 24 ($n = 6$ mice per time point for WT and $n = 4$ mice per time point for *Cry1*$^{-/-}$ *Cry2*$^{-/-}$; equal numbers of male and female mice were used for each group). SMG tissue was kept in a freezer at −80 °C with TRIzol reagent (Life Technologies) until later use.

Preparation of SMG cultures at ZT 0 and ZT 12

For ex vivo experiments, male 2–3 month-old PER2::LUC mice were euthanized by cervical dislocation under anesthesia at ZT 0 or 12, and SMGs were rapidly placed in chilled HBSS and dissected into approximately 24 sections. Sections were equally divided into six dishes, which were maintained in the dark in an incubator at 35 °C. Sectioned SMGs were collected at 8, 12, 16, 20, 24, and 28 h after each preparation at ZT 0 or ZT 12 ($n = 4$–6); collection of samples of the ZT 0 preparation were started at the projected ZT 8 and that of samples of the ZT 12 preparation at the projected ZT 20. SMG tissue was kept in a freezer at −80 °C with TRIzol reagent (Life Technologies) until later use.

RNA isolation and real-time quantitative RT-PCR

Total RNA was isolated from the SMG using TRIzol reagent and a PureLink RNA Mini kit (Life Technologies) and reverse-transcribed using a PrimeScript RT Reagent kit (TaKaRa BIO Inc.; Otsu, Shiga, Japan) according to the manufacturers' instructions. Quantitative PCR analysis of the individual cDNAs was performed using the iQ SYBR Green Supermix (Bio-Rad, Hercules, CA). PCR cycling was performed for 40 cycles (at 95 °C for 10 s and 55 °C for 30 s) using a MyiQ Single Color Real-Time PCR Detection System (Bio-Rad) and the following PCR primers: *Actb* (FW: 5′-ctcttttccagccttccttc-3′, RV: 5′-atctccttctgcatcctgtc-3′); *Per2* (FW: 5′-ccagaggaactagcctataagaacca-3′, RV: 5′-gaactcgcacttcctttcagg-3′ [26]); *Bmal1* (FW: 5′-cagtgccactgactaccaagaaa-3′, RV: 5′-cctcccaagcattcttgatcc-3′ [26]; *Dbp* (FW: 5′-aggaactgaagcctcaaccaatc-3′, RV: 5′-ctccggctccagtacttctcat-3′ [26]); *Aqp5* (FW: 5′-ggccctcttaataggcaacc-3′, RV: 5′-ttgcctggtgttgtgttgtt-3′ [25]).

Quantitative reverse transcriptase (RT)-PCR results were normalized to *Actb* mRNA levels, and a relative quantification of mRNA was determined using the ΔCT method. The CT value of target genes was subtracted from that of *Actb* at each time point using the following formula:

$$\Delta CT = CT \text{ target gene} - CT\textit{Actb}.$$

$2^{-\Delta CT}$ indicated the relative expression level of the target gene mRNA, normalized to the mean value of the mRNA level in WT mice, with levels expressed as the relative intensity at each point.

Statistics

For the bioluminescence analyses, one-way analysis of variance (ANOVA) was used to compare the period length and the first peak phase of PER2::LUC activity in the SMGs of WT, *Cry1*$^{-/-}$, and *Cry2*$^{-/-}$ mice. For mRNA expression profile analysis, one-way ANOVA was used to detect the difference in the time-dependent expression levels of each gene.

Results

Localization of PER2::LUC activity in the mouse SMG

To localize the molecular clock component in the mouse SMG, we first obtained bioluminescence images of

PER2::LUC activity in this region. Bright-field images revealed the acinus of the SMG and delineated lumens of the associated ducts (Fig. 1a). PER2 expression was strongly detected in acinar cells and showed robust fluctuation in acini. The circadian change in PER2::LUC activity was also observed in an SMG slice (Fig. 1b).

Circadian rhythms of PER2::LUC activity in the SMG were associated with mouse genotype

The circadian rhythms of PER2::LUC activity were examined to determine whether the molecular clock also oscillates in cultured SMG ex vivo. PER2::LUC activity in the SMGs of WT and *Cry2*$^{-/-}$ mice was robustly rhythmic and persisted for >5 days (Fig. 2a, left and right graphs), while that in the SMGs of *Cry1*$^{-/-}$ mice showed a similar circadian rhythmicity but with a more rapid dampening of the rhythm (Fig. 2a, middle graph). The SMG of each genotype had its own characteristic period (Fig. 2b) and phase (Fig. 2c). The average period of *Cry1*$^{-/-}$ SMGs [mean ± standard deviation (SD) 20.3 ± 0.4 h) was significantly shorter than that of WT SMGs (23.0 ± 0.8 h), while that of *Cry2*$^{-/-}$ SMGs (25.1 ± 0.8 h) was significantly longer (Fig. 2b; one-way ANOVA, $p < 0.01$). The first peak after culturing was at 29.9 ± 0.8 h in WT SMGs, 23.9 ± 1.2 h in *Cry1*$^{-/-}$ SMGs, and 37.9 ± 3.4 h in *Cry2*$^{-/-}$ SMGs (Fig. 2c). The differences in peak phase showed statistical significance (one-way ANOVA, $p < 0.01$).

Daily fluctuations in *Per2, Bmal1, Dbp*, and *Aqp5* mRNA levels in the SMG were disrupted in *Cry1*$^{-/-}$ *Cry2*$^{-/-}$ mice

To investigate whether the expression of the major clock genes *Per2* and *Bmal1* and the clock-controlled gene *Dbp* oscillates in the SMG, we measured the expression levels of these genes throughout the day by quantitative RT-PCR using samples collected in vivo. Because no differences were observed with regard to the sex of the mice, we analyzed data with mixed samples that included equal numbers of male and female mice for each time point. *Per2* mRNA in the SMG of WT mice showed diurnal variation (Fig. 3a, left graph; one-way ANOVA, $p < 0.001$), as did *Bmal1* and *Dbp* mRNA (Fig. 3b, c, left graph; one-way ANOVA, *Bmal1*: $p < 0.001$; *Dbp*: $p < 0.001$). In contrast, the expression of *Per2*, *Bmal1*, and *Dbp* mRNA in the SMG of *Cry1*$^{-/-}$ *Cry2*$^{-/-}$ mice did not show significant variations (Fig. 3a–c, right graph; one-way ANOVA, *Per2*: $p = 0.800$; *Bmal1*: $p = 0.822$; *Dbp*: $p = 0.307$). Compared with rhythms in WT mice, the expression levels of *Per2* and *Dbp* mRNA were highly consistent throughout the day in *Cry1*$^{-/-}$ *Cry2*$^{-/-}$ mice while, in contrast, the expression of *Bmal1* mRNA was depressed throughout the day in *Cry1*$^{-/-}$ *Cry2*$^{-/-}$ mice. We also examined the diurnal variation of *Aqp5* mRNA expression in the SMG of WT and *Cry1*$^{-/-}$ *Cry2*$^{-/-}$ mice in vivo and observed that *Aqp5* mRNA expression in the SMG of WT mice showed diurnal variations (Fig. 3d, left graph; one-way ANOVA, $p = 0.037$), but did not vary in the SMG of *Cry1*$^{-/-}$ *Cry2*$^{-/-}$ mice (Fig. 3d, right graph; one-way ANOVA, $p = 0.994$).

Circadian rhythms were detected in the expression of *Per2, Bmal1*, and *Dbp mRNA*, but not in that of *Aqp5* mRNA in cultured SMGs

The SMGs of WT mice were cultured and the tissue collected at projected ZT 0, 4, 8, 12, 16 and 20. Expression of *Per2*, *Bmal1*, and *Dbp* mRNA showed circadian rhythm-associated variations (Fig. 4a–c; one-way ANOVA, *Per2*: $p < 0.001$; *Bmal1*: $p < 0.001$; *Dbp*: $p < 0.001$). The

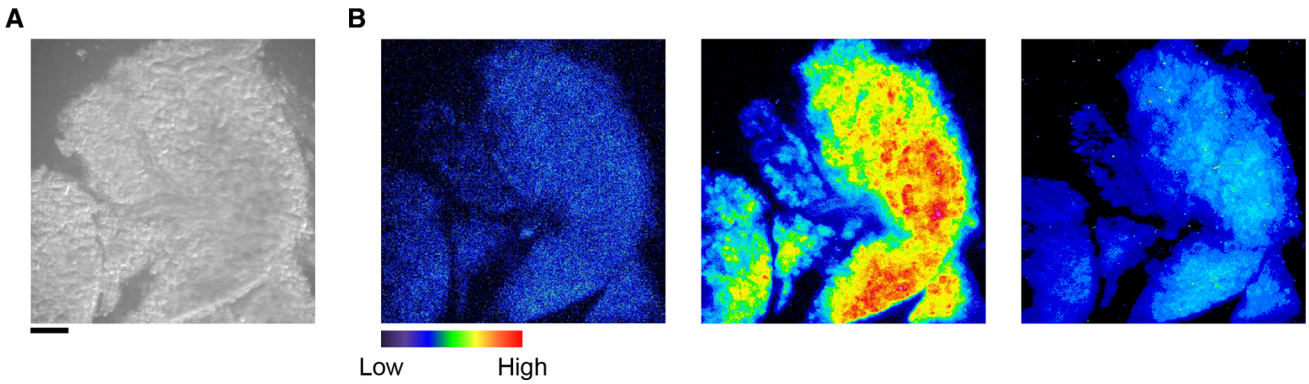

Fig. 1 Abundant expression of the PERIOD2::LUCIFERASE fusion protein (PER2::LUC) in the acinus of the submandibular gland (SMG) except for the ductal lumens. **a**, **b** Representative bright-field (**a**) and bioluminescence (**b**) images at the first trough (*left*), first peak (*middle*), and second trough (*right*) in the SMG of a PER2::LUC mouse. *Scale bar* 250 μm, *pseudocolor bar* relative intensity of PER2::LUC activity

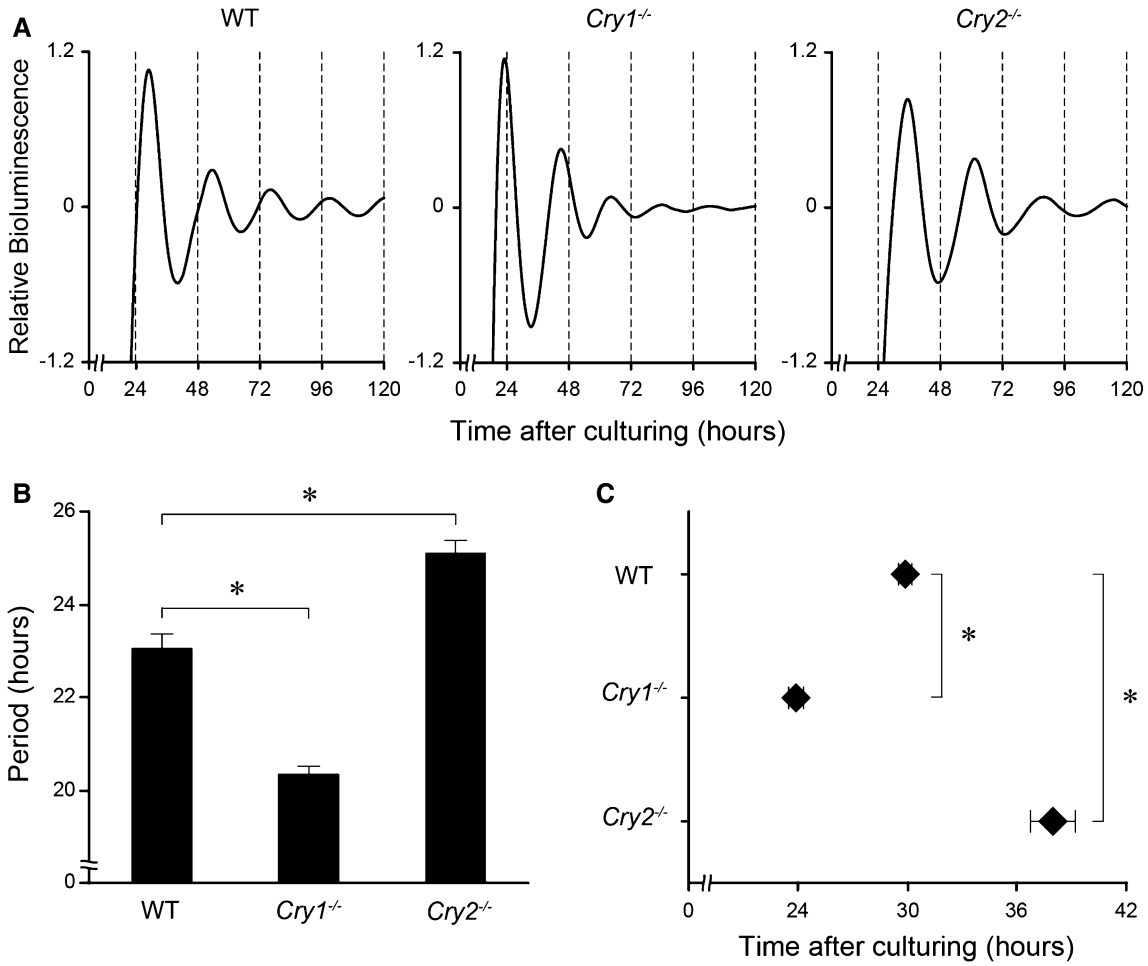

Fig. 2 Circadian rhythms in PER2::LUC in cultured SMGs of wild-type (*WT*), *Cry1*$^{-/-}$, and *Cry2*$^{-/-}$ mice ex vivo. **a** Representative bioluminescence oscillations showing PER2::LUC activity in the SMG of WT (*left*), *Cry1*$^{-/-}$ (*middle*), and *Cry2*$^{-/-}$ (*right*) mice. Hours, starting from the time when tissues were cultured, are displayed on the *X-axis*. Serial de-trended bioluminescence counts are plotted for 5 days. **b** Circadian periods of PER2::LUC rhythms in the SMG of each genotype. **c** The first peak phase of PER2::LUC rhythms in the SMG of each genotype. All values are the mean ± standard deviation ($n = 8$ in each genotype). * $P < 0.01$ (vs. WT, Scheffé post hoc test)

expression profiles of *Aqp5* mRNA from ZT 0 and ZT 12 preparations showed a two-peak variation along a 24-h time course (Fig. 4d). However, individual plots did not show any circadian fluctuations although they revealed a steady shrinking over time regardless of preparation time (Fig. 4e, f; one-way ANOVA, ZT 0: $p < 0.001$; ZT 12: $p < 0.001$).

Discussion

We observed that the rhythms of the major clock genes *Per2* and *Bmal1* and the clock-controlled gene *Dbp* oscillate in SMGs collected both in vivo and ex vivo in a manner dependent on the expression of *Cry1* and *Cry2*. These results were confirmed by bioluminescence recordings of PER2::LUC activity. Moreover, the circadian and diurnal rhythms of these clock genes were associated with the phenotype of *Cry1*$^{-/-}$, *Cry2*$^{-/-}$, and *Cry1*$^{-/-}$ *Cry2*$^{-/-}$ mice. These data support the hypothesis that the SMG has self-sustaining oscillators driven by the molecular clock. We also observed rhythmic expression of *Aqp5* mRNA in vivo, but not ex vivo. The observation that the circadian rhythmicity of *Aqp5* mRNA expression disappeared in cultured SMGs suggests that its rhythm within the SMG is predominantly driven by the master clock in the SCN via several pathways. These potentially include the circadian rhythms in the autonomic nervous system governed by the SCN [34] and indirectly through feeding rhythms that accompany metabolic changes and mechanical stimuli [21].

In mammals, the existence of a tissue-autonomous peripheral clock was proposed based on the circadian rhythm in the biological response of mouse adrenal glands

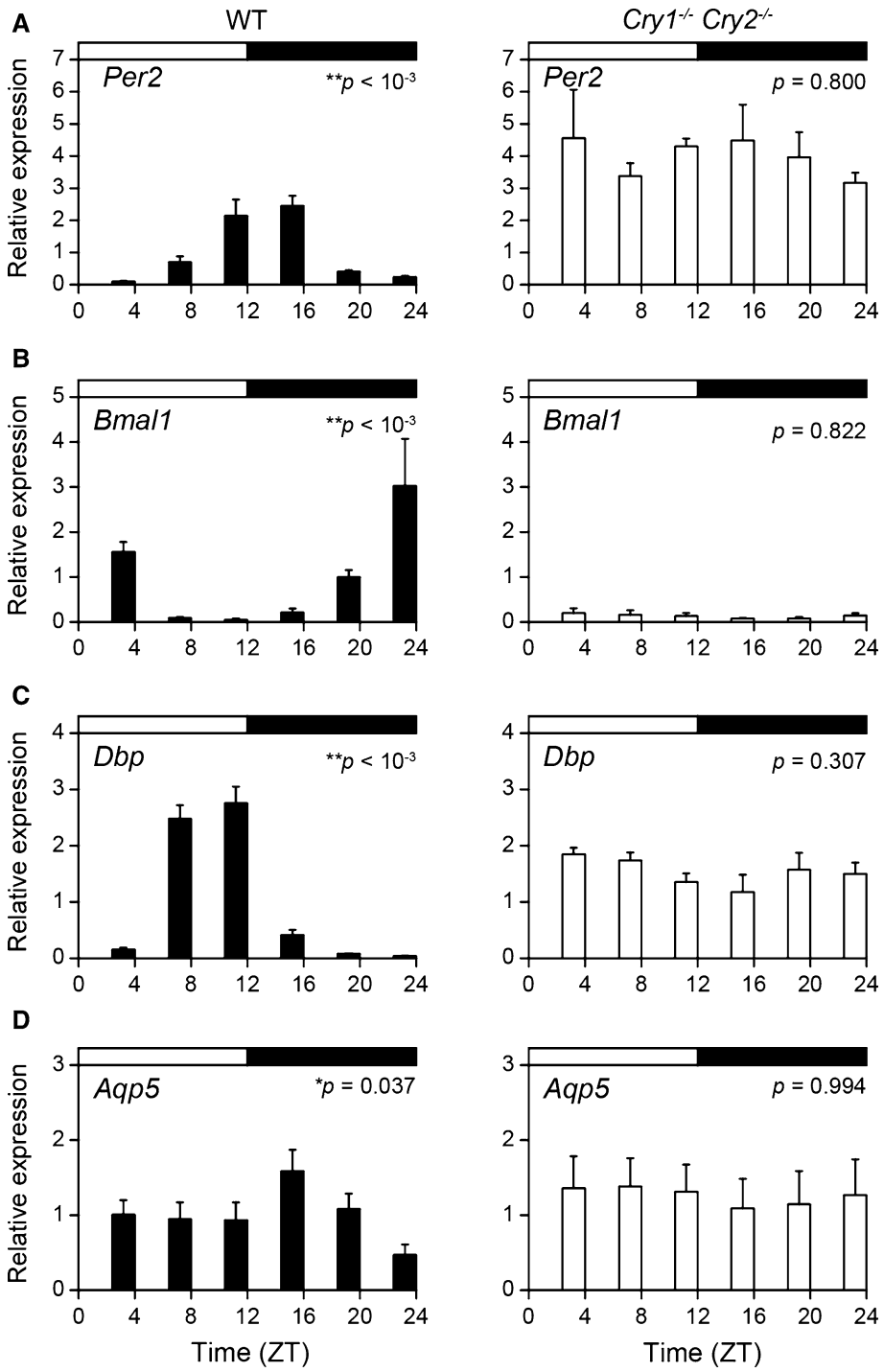

Fig. 3 Daily expression profiles of clock genes *Per2* and *Bmal1*, clock-controlled gene *Dbp*, and aquaporin-5 (*Aqp5*) mRNA in the SMGs of $Cry1^{-/-}$ $Cry2^{-/-}$ mice collected in vivo. **a–d** *Per2* (**a**), *Bmal1* (**b**), *Dbp* (**c**), and *Aqp5* (**d**) mRNA expression levels in the SMGs of WT mice (*black columns*) and $Cry1^{-/-}$ $Cry2^{-/-}$ mice (*white columns*). The *black* and *white horizontal bar at the top of each graph* indicates the dark and light phases, respectively. Data are shown as mean ± standard error of the mean (SEM) ($n = 6$ WT mice per time point and $n = 4$ $Cry1^{-/-}$ $Cry2^{-/-}$ mice per time point). Significance of the analysis of variance: $*p < 0.05$, $**p < 0.01$. *ZT* Zeitgeber time

ex vivo [35]. Cultured hamster retinas that exhibited circadian rhythms of melatonin synthesis in vitro with periods dependent on circadian genotypes provided direct evidence for these peripheral clocks [36]. $Cry1^{-/-}$ and $Cry2^{-/-}$ mice exhibit a shorter and longer free-running period, respectively, than WT mice [28]. Furthermore, $Cry1^{-/-}$ $Cry2^{-/-}$ mice, which lack a circadian clock, show arrhythmic behavior, physiology, and metabolism [28, 37]. In the present study, we examined PER2::LUC rhythms in the SMG of WT, $Cry1^{-/-}$, and $Cry2^{-/-}$ mice and compared period lengths. We observed that the circadian rhythms in the SMG were altered in $Cry1^{-/-}$ and $Cry2^{-/-}$ mice. Compared with WT mice, the period length was shorter in $Cry1^{-/-}$ mice, while the period was longer in $Cry2^{-/-}$ mice. These data are consistent with the behavioral phenotypes of $Cry1^{-/-}$ and $Cry2^{-/-}$ mice, as well as with the

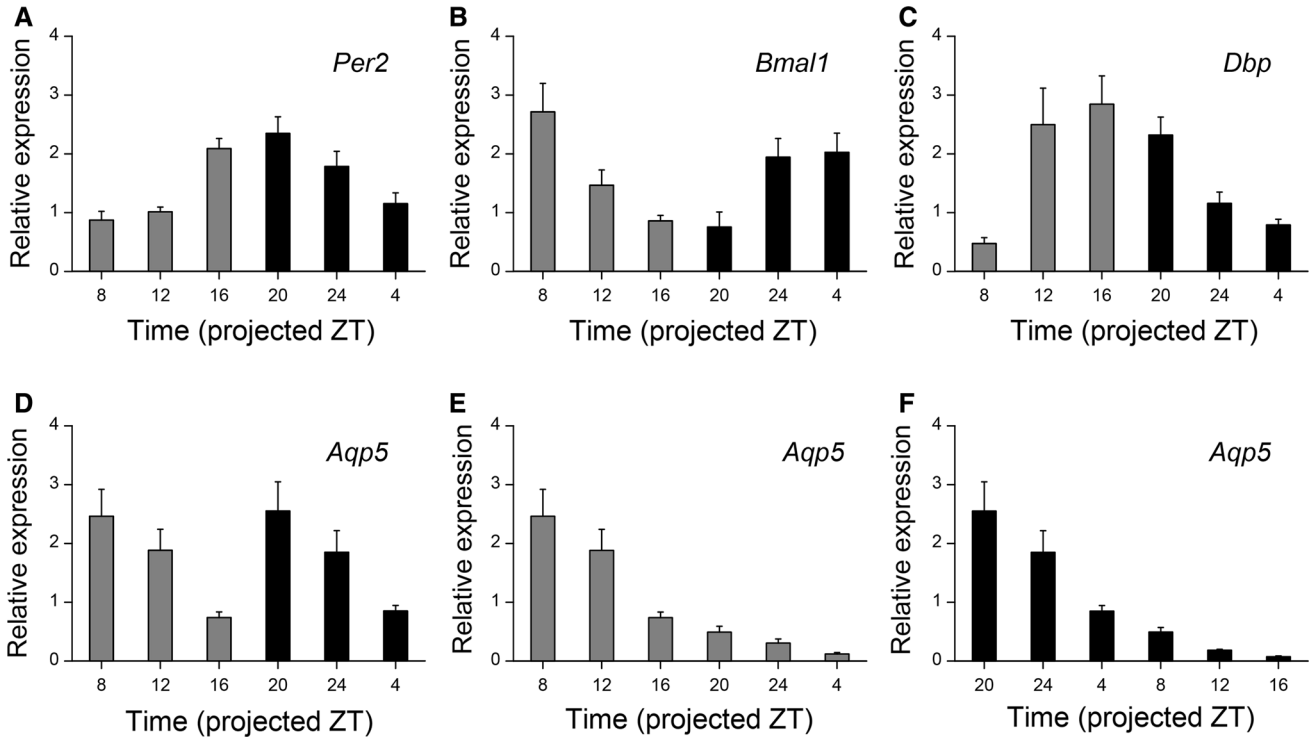

Fig. 4 Circadian expression profiles of *Per2*, *Bmal1*, *Dbp*, and *Aqp5* mRNA in cultured SMGs ex vivo. **a–c** *Per2* (**a**), *Bmal1* (**b**), and *Dbp* (**c**) mRNA expression levels in SMG cultures prepared at ZT 0 (*gray column*) and ZT 12 (*black column*). Samples at ZT 8, 12, and 16 were collected from a ZT 0 preparation, and samples from ZT 20, 24, and 4 were collected from a ZT 12 preparation. **d–f** *Aqp5* mRNA expression levels in samples (**d**) prepared at ZT 0 (**e**) and ZT 12 (**f**). Samples were collected at the projected ZTs described on each chart. Data are shown as mean ± SEM ($n = 5$ mice per time point in ZT 0 preparation and $n = 6$ mice per time point in ZT 12 preparation)

results of a previous study that described PER2::LUC rhythms in SCN explants from *Cry1*$^{-/-}$ and *Cry2*$^{-/-}$ mice [20, 38]. We observed robust PER2::LUC activity in the acini of the SMG. The localization of the expression of clock genes was consistent with a previous study that reported the expression of these genes in the three major types of salivary glands [30]. Furthermore, previous studies demonstrated that AQP5 expression is localized in acinar cells in human, rat, and mouse salivary glands. These findings suggest that salivation is related to the molecular clock composed of clock genes [15, 39, 40].

The mRNA expression profiles of *Per2*, *Bmal1*, and *Dbp* from in vivo experiments in the SMG showed daily rhythms. The rhythms of *Per2* and *Bmal1* mRNA expression were anti-phase with respect to each other. In contrast, the expression profiles in the SMGs of *Cry1*$^{-/-}$ *Cry2*$^{-/-}$ mice did not show rhythmicity, with *Per2* mRNA expressed at consistently high levels and *Bmal1* mRNA expressed at consistently low levels throughout the day. These results are consistent with a previous study examining those expression profiles in the adrenal glands of *Cry1*$^{-/-}$ *Cry2*$^{-/-}$ mice [37]. Furthermore, we examined the expression profiles of *Per2* and *Bmal1* in cultured SMGs ex vivo, which were isolated from, and not affected by, autonomic innervation or variations in body temperature and feeding. In the ex vivo experiments, the mRNA expression profiles of *Per2* and *Bmal1* also showed circadian rhythms and were anti-phase with respect to each other. These results indicate that cultured SMGs remained healthy throughout the sampling course of our study. *Dbp* is a clock-controlled gene containing an E-box motif in the promoter region, and its expression shows circadian rhythms through E-box regulation [41]. In the present study, expression of *Dbp* mRNA in the SMGs of WT mice showed circadian rhythms in samples collected both in vivo and ex vivo. In contrast, in the SMGs of *Cry1*$^{-/-}$ *Cry2*$^{-/-}$ mice, *Dbp* mRNA was expressed at consistently high levels throughout the day. These results reveal that the expression of *Dbp* in the SMG is dependent on E-box regulation. Taken together, these results suggest that the SMG has self-sustaining oscillators driven by TTFLs.

Previous studies have demonstrated that AQP5 plays an important role in water permeability in the salivary glands [16, 42]. In our study, expression of *Aqp5* mRNA in the SMG of WT mice showed significant daily variation in vivo, and its acrophase was observed at midnight (ZT 16) during the active phase in mice. In the SMGs of *Cry1*$^{-/-}$ *Cry2*$^{-/-}$ mice, *Aqp5* mRNA was expressed at intermediate levels throughout the day. These results indicate that the expression of *Aqp5* is affected by the

circadian system. However, *Aqp5* mRNA did not show any circadian fluctuation in ex vivo experiments, indicating that in cultured SMGs, expression of *Aqp5* mRNA was no longer predominantly regulated by cell-autonomous oscillations. Therefore, exhaustive analysis in salivary glands may provide the important information for the circadian regulation of *Aqp5* in vivo [43]. In contrast to the decline of *Aqp5* rhythmicity in cultured SMGs, in vitro circadian rhythms were reported for melatonin synthesis in the retina [36] and reactivity to adrenocorticotropic hormone in the adrenal glands [35], which could be under the control of cell-autonomous oscillations. In a study conducted in sympathectomized rats, the phase of *Per1* expression in denervated SMG entrained robustly to the feeding schedule, although with an intact SMG, the phase mostly entrained to light-dark cycle information via the autonomic nervous system [44]. On the other hand, the results from a previous study suggest that the circadian variation in mucin secretion from respiratory submucosal glands is under the control of the SCN via vagal nerve [45]. Taken together, these results indicate that the daily rhythm of *Aqp5* expression is predominantly controlled by the central clock in the SCN via the autonomic pathway, feeding, and other entrainment factors under normal conditions, whereas denervated and/or isolated conditions, such as ex vivo culture conditions, lead to a decline in rhythmicity.

In summary, our study demonstrates that the mouse SMG contains self-sustaining circadian oscillators driven by TTFLs. Although the circadian expression of *Aqp5* has been proposed to be directly regulated by TTFLs [30], our ex vivo data suggest that it is predominantly driven by the master clock in the SCN via the autonomic nervous system. Further studies are necessary to elucidate the regulatory mechanisms that control the circadian expression of functional molecules in the SMG.

Author contributions H.U. and W.N. designed the research; H.U., T.J.N., N.N.T., and W.N. performed the research; A.O.K., H.O., T.T., and T.S. contributed new reagents/analytic tools; H.U., T.J.N., N.N.T., and W.N. analyzed the data; H.U., T.J.N., N.N.T., and W.N. wrote the paper.

Compliance with ethical standards

Conflict of interest The authors declare that they have no conflict of interest.

Funding This work was supported by JSPS KAKENHI grant numbers 26462809, 26860160, 26861780. N.N.T. is a research fellow of the Japan Society for the Promotion of Science.

Ethical approval All applicable international, national, and/or institutional guidelines for the care and use of animals were followed. The Protocol was approved by the Animal Care and Use Committee at Osaka University.

References

1. Brosky ME (2007) The role of saliva in oral health: strategies for prevention and management of xerostomia. J Support Oncol 5:215–225
2. Rudney JD (1995) Does variability in salivary protein concentrations influence oral microbial ecology and oral health? Crit Rev Oral Biol Med 6:343–367
3. Cohen S (1962) Isolation of a mouse submaxillary gland protein accelerating incisor eruption and eyelid opening in the new-born animal. J Biol Chem 237:1555–1562
4. Levine MJ (1993) Development of artificial salivas. Crit Rev Oral Biol Med 4:279–286
5. Schneyer LH, Levin LK (1955) Rate of secretion by individual salivary gland pairs of man under conditions of reduced exogenous stimulation. J Appl Physiol 7:508–512
6. Abe K, Dawes C (1978) The effects of electrical and pharmacological stimulation on the types of proteins secreted by rat parotid and submandibular glands. Arch Oral Biol 23:367–372
7. Garrett JR, Suleiman AM, Anderson LC, Proctor GB (1991) Secretory responses in granular ducts and acini of submandibular glands in vivo to parasympathetic or sympathetic nerve stimulation in rats. Cell Tissue Res 264:117–126
8. Garrett JR, Thulin A (1975) Changes in parotid acinar cells accompanying salivary secretion in rats on sympathetic or parasympathetic nerve stimulation. Cell Tissue Res 159:179–193
9. Dawes C (1972) Circadian rhythms in human salivary flow rate and composition. J Physiol 220:529–545
10. Siminoski K, Bernanke J, Murphy RA (1993) Nerve growth factor and epidermal growth factor in mouse submandibular glands: identical diurnal changes and rates of secretagogue-induced synthesis. Endocrinology 132:2031–2037
11. Basso A, Piantanelli L (2002) Influence of age on circadian rhythms of adrenoceptors in brain cortex, heart and submandibular glands of BALB/c mice: when circadian studies are not only useful but necessary. Exp Gerontol 37:1441–1450
12. Agre P, King LS, Yasui M, Guggino WB, Ottersen OP, Fujiyoshi Y, Engel A, Nielsen S (2002) Aquaporin water channels–from atomic structure to clinical medicine. J Physiol 542:3–16
13. Castle NA (2005) Aquaporins as targets for drug discovery. Drug Discov Today 10:485–493
14. Verkman AS (2005) More than just water channels: unexpected cellular roles of aquaporins. J Cell Sci 118:3225–3232
15. Delporte C, Steinfeld S (2006) Distribution and roles of aquaporins in salivary glands. Biochim Biophys Acta 1758:1061–1070
16. Ma T, Song Y, Gillespie A, Carlson EJ, Epstein CJ, Verkman AS (1999) Defective secretion of saliva in transgenic mice lacking aquaporin-5 water channels. J Biol Chem 274:20071–20074
17. Yang B, Song Y, Zhao D, Verkman AS (2005) Phenotype analysis of aquaporin-8 null mice. Am J Physiol Cell Physiol 288:C1161–C1170
18. Nakamura TJ, Takasu NN, Nakamura W (2016) The suprachiasmatic nucleus: age-related decline in biological rhythms. J Physiol Sci 66:367–374
19. Abe M, Herzog ED, Yamazaki S, Straume M, Tei H, Sakaki Y, Menaker M, Block GD (2002) Circadian rhythms in isolated brain regions. J Neurosci 22:350–356
20. Uchida H, Nakamura TJ, Takasu NN, Todo T, Sakai T, Nakamura W (2016) Cryptochrome-dependent circadian periods in the arcuate nucleus. Neurosci Lett 610:123–128
21. Tahara Y, Kuroda H, Saito K, Nakajima Y, Kubo Y, Ohnishi N, Seo Y, Otsuka M, Fuse Y, Ohura Y et al (2012) In vivo monitoring of peripheral circadian clocks in the mouse. Curr Biol 22:1029–1034

22. Yamazaki S, Numano R, Abe M, Hida A, Takahashi R, Ueda M, Block GD, Sakaki Y, Menaker M, Tei H (2000) Resetting central and peripheral circadian oscillators in transgenic rats. Science 288:682–685
23. Yoo SH, Yamazaki S, Lowrey PL, Shimomura K, Ko CH, Buhr ED, Siepka SM, Hong HK, Oh WJ, Yoo OJ et al (2004) PERIOD2:LUCIFERASE real-time reporting of circadian dynamics reveals persistent circadian oscillations in mouse peripheral tissues. Proc Natl Acad Sci USA 101:5339–5346
24. Reppert SM, Weaver DR (2002) Coordination of circadian timing in mammals. Nature 418:935–941
25. Inouye ST, Kawamura H (1979) Persistence of circadian rhythmicity in a mammalian hypothalamic "island" containing the suprachiasmatic nucleus. Proc Natl Acad Sci USA 76:5962–5966
26. Meyer-Bernstein EL, Jetton AE, Matsumoto SI, Markuns JF, Lehman MN, Bittman EL (1999) Effects of suprachiasmatic transplants on circadian rhythms of neuroendocrine function in golden hamsters. Endocrinology 140:207–218
27. Schwartz WJ, Gross RA, Morton MT (1987) The suprachiasmatic nuclei contain a tetrodotoxin-resistant circadian pacemaker. Proc Natl Acad Sci USA 84:1694–1698
28. Vitaterna MH, Selby CP, Todo T, Niwa H, Thompson C, Fruechte EM, Hitomi K, Thresher RJ, Ishikawa T, Miyazaki J et al (1999) Differential regulation of mammalian period genes and circadian rhythmicity by cryptochromes 1 and 2. Proc Natl Acad Sci USA 96:12114–12119
29. Furukawa M, Kawamoto T, Noshiro M, Honda KK, Sakai M, Fujimoto K, Honma S, Honma K, Hamada T, Kato Y (2005) Clock gene expression in the submandibular glands. J Dent Res 84:1193–1197
30. Zheng L, Seon YJ, McHugh J, Papagerakis S, Papagerakis P (2012) Clock genes show circadian rhythms in salivary glands. J Dent Res 91:783–788
31. Nakamura TJ, Nakamura W, Tokuda IT, Ishikawa T, Kudo T, Colwell CS, Block GD (2015) Age-related changes in the circadian system unmasked by constant conditions. eNeuro 2(4). doi:10.1523/ENEURO.0064-15.2015
32. Sakai T, Larsen M, Yamada KM (2003) Fibronectin requirement in branching morphogenesis. Nature 423:876–881
33. Nakamura W, Yamazaki S, Takasu NN, Mishima K, Block GD (2005) Differential response of Period 1 expression within the suprachiasmatic nucleus. J Neurosci 25:5481–5487
34. Ueyama T, Krout KE, Nguyen XV, Karpitskiy V, Kollert A, Mettenleiter TC, Loewy AD (1999) Suprachiasmatic nucleus: a central autonomic clock. Nat Neurosci 2:1051–1053
35. Ungar F, Halberg F (1962) Circadian rhythm in the in vitro response of mouse adrenal to adrenocorticotropic hormone. Science 137:1058–1060
36. Tosini G, Menaker M (1996) Circadian rhythms in cultured mammalian retina. Science 272:419–421
37. Doi M, Takahashi Y, Komatsu R, Yamazaki F, Yamada H, Haraguchi S, Emoto N, Okuno Y, Tsujimoto G, Kanematsu A et al (2010) Salt-sensitive hypertension in circadian clock-deficient Cry-null mice involves dysregulated adrenal Hsd3b6. Nat Med 16:67–74
38. Evans JA, Pan H, Liu AC, Welsh DK (2012) Cry1$^{-/-}$ circadian rhythmicity depends on SCN intercellular coupling. J Biol Rhythms 27:443–452
39. Gresz V, Kwon TH, Hurley PT, Varga G, Zelles T, Nielsen S, Case RM, Steward MC (2001) Identification and localization of aquaporin water channels in human salivary glands. Am J Physiol Gastrointest Liver Physiol 281:G247–G254
40. Matsuzaki T, Ablimit A, Suzuki T, Aoki T, Hagiwara H, Takata K (2006) Changes of aquaporin 5-distribution during release and reaccumulation of secretory granules in isoproterenol-treated mouse parotid gland. J Electron Microsc (Tokyo) 55:183–189
41. Ueda HR, Hayashi S, Chen W, Sano M, Machida M, Shigeyoshi Y, Iino M, Hashimoto S (2005) System-level identification of transcriptional circuits underlying mammalian circadian clocks. Nat Genet 37:187–192
42. Krane CM, Melvin JE, Nguyen HV, Richardson L, Towne JE, Doetschman T, Menon AG (2001) Salivary acinar cells from aquaporin 5-deficient mice have decreased membrane water permeability and altered cell volume regulation. J Biol Chem 276:23413–23420
43. Koike N, Yoo SH, Huang HC, Kumar V, Lee C, Kim TK, Takahashi JS (2012) Transcriptional architecture and chromatin landscape of the core circadian clock in mammals. Science 338:349–354
44. Vujovic N, Davidson AJ, Menaker M (2008) Sympathetic input modulates, but does not determine, phase of peripheral circadian oscillators. Am J Physiol Regul Integr Comp Physiol 295:R355–R360
45. Bnado H, Nishio T, van der Horst GTJ, Masubuchi S, Hisa Y, Okamura H (2007) Vagal regulation of respiratory clocks in mice. J Neurosci 27:4359–4365